

Nuclear Ca^{2+} concentration measured with specifically targeted recombinant aequorin

Marisa Brini¹, Marta Murgia, Lucia Pasti, Didier Picard², Tullio Pozzan and Rosario Rizzuto

Department of Biomedical Sciences and CNR Center for the Study of Mitochondrial Physiology, University of Padova, Via Trieste 75, 35121 Padova, Italy and ²Département de Biologie Cellulaire, Université de Genève, Sciences III, 30 Quai Ernest-Ansermet, CH-1211 Genève, Switzerland

¹Corresponding author

Communicated by T.Pozzan

Activation of nuclear transcription factors, breakdown of nuclear envelope and apoptosis represent a group of nuclear events thought to be modulated by changes in nucleoplasmic Ca^{2+} concentration, $[\text{Ca}^{2+}]_n$. Direct evidence for, or against, this possibility has been, however, difficult to obtain because measurements of $[\text{Ca}^{2+}]_n$ are hampered by major technical problems. Here we describe a new approach for selectively monitoring Ca^{2+} concentrations inside the nucleus of living cells, which is based on the construction of a chimeric cDNA encoding a fusion protein composed of the photoprotein aequorin and a nuclear translocation signal derived from the rat glucocorticoid receptor. This modified aequorin (nuAEQ), stably expressed in HeLa cells, was largely confined to the nucleoplasm and thus utilized for monitoring $[\text{Ca}^{2+}]_n$ in intact cells. No significant differences were observed between $[\text{Ca}^{2+}]_n$ and cytosolic Ca^{2+} concentration ($[\text{Ca}^{2+}]_i$) under resting conditions. Upon stimulation of surface receptors linked to inositol-1,4,5-trisphosphate (InsP3) generation, and thus to intracellular Ca^{2+} signalling, the kinetics of $[\text{Ca}^{2+}]_i$ and $[\text{Ca}^{2+}]_n$ increases were indistinguishable. However, for the same rise in $[\text{Ca}^{2+}]_i$, the amplitude of $[\text{Ca}^{2+}]_n$ increase was larger when evoked by Ca^{2+} mobilization from internal stores than when induced by Ca^{2+} influx across the plasma membrane. The functional significance of these transient nucleus–cytosol Ca^{2+} gradients is discussed.

Key words: aequorin/calcium/fura-2/nucleus/signal transduction

Introduction

The intracellularly trappable Ca^{2+} indicators, such as quin2, fura-2, indo-1, etc. (Tsien *et al.*, 1982; Grynkiewicz *et al.*, 1985), have been invaluable tools in providing evidence for a pivotal role of calcium ions in transducing inside the cell a wide variety of external stimuli (Berridge and Irvine, 1989; Tsien, 1989; Meldolesi *et al.*, 1990). The Ca^{2+} signal exhibits a high degree of spatio-temporal complexity, whose significance and mechanism are, however, only partially understood. In this context, intracellular organelles play a key role. On the one hand,

subcellular structures accumulate (and release upon cell stimulation) calcium ions, thereby contributing to the control of cytosolic Ca^{2+} concentration ($[\text{Ca}^{2+}]_i$); on the other hand, $[\text{Ca}^{2+}]$ inside organelles, such as mitochondria, endoplasmic reticulum and nucleus, modulates their specific functions, suggesting therefore that these structures are indeed targets of the Ca^{2+} signal.

Nucleoplasmic Ca^{2+} concentration ($[\text{Ca}^{2+}]_n$) has been recently proposed to be involved in the regulation of key nuclear processes, such as gene expression, breakdown of nuclear envelope and apoptosis (Collart *et al.*, 1991; Gaido and Cidlowski, 1991; Tombes *et al.*, 1992). The study of the relationship between $[\text{Ca}^{2+}]_i$ and $[\text{Ca}^{2+}]_n$, however, depends on the possibility of specifically measuring these two parameters in living cells. The fluorescent Ca^{2+} indicators are not ideally suited for that purpose. They are in fact trapped in the cytoplasm of intact cells because the esterases (which hydrolyse the acetoxymethylester) are primarily, if not exclusively, localized in the cytosol (Tsien *et al.*, 1982; Malgaroli *et al.*, 1987). The possibility of measuring $[\text{Ca}^{2+}]_n$ with these probes depends on their permeability through the nuclear envelope (and/or the presence of esterases in the nucleoplasm) and on the availability of techniques capable of distinguishing the signal originating from the two compartments. Contradictory data exist in the literature about these issues. The nuclear membrane is generally considered freely permeable to solutes up to 10–20 kDa (Lange *et al.*, 1986); no barrier to the diffusion of the Ca^{2+} indicators (MW \approx 1000 Da) into the nucleus should therefore exist. Local accumulation or exclusion of the dyes in/from the nucleus has been, however, noticed (Williams *et al.*, 1985; Connor, 1993). It has even been reported that isolated nuclei hydrolyse fura-2/AM and trap the acid form, suggesting that in living cells, they are impermeable to the dyes generated in the cytoplasm (Nicotera *et al.*, 1989). Also assuming that the nucleus is permeable to the Ca^{2+} indicators generated or injected in the cytoplasm, the problem that the signal coming from the nucleus is always contaminated by that of the surrounding cytosol is inescapable, at least with classical image analysis. Quantitative confocal microscopy studies of $[\text{Ca}^{2+}]_n$ are very few to date and they too appear subject to some of the above mentioned criticisms (Birch *et al.*, 1992; Himpens *et al.*, 1992).

We have recently described a new strategy for monitoring Ca^{2+} concentration in subcellular compartments of intact cells (Rizzuto *et al.*, 1992). This method takes advantage of the possibility of directing the Ca^{2+} -sensitive luminescent protein, aequorin, to defined subcellular locations, by modifying its cDNA in order to include organelle-specific targeting sequences. The first of such chimeric aequorins was selectively targeted to the mitochondria and the matrix Ca^{2+} concentration could thus be measured in intact transfected cells (Rizzuto *et al.*, 1992). A similar strategy was employed here for specifically targeting aequorin to the

nucleus of intact cells: the engineered photoprotein, expressed in HeLa cells, permitted the first direct measurement of nucleoplasmic Ca^{2+} concentration *in situ*.

Results

Design and expression of nuclear-targeted chimeric aequorin

The strategy for designing a cDNA coding for nuclear targeted aequorin is described in Figure 1. In particular, in order to obtain constitutive targeting to the nucleus, part of the rat glucocorticoid receptor (GR) cDNA, including a nuclear localization signal, was fused in-frame with a portion of the aequorin cDNA encoding virtually the whole photoprotein (only the first amino acid of wild-type aequorin is missing from the chimeric polypeptide). The GR cDNA moiety encoded amino acids 407–524, which includes the DNA binding domain and the nuclear localization signal NL1 (Picard and Yamamoto, 1987) of GR. In order to prevent interference with the luminescence properties of aequorin (Nomura *et al.*, 1991), the GR sequence was added to the N-terminus of the protein. Essentially the same portion of GR (aa 407–545) has previously been shown to mediate constitutive nuclear localization of β -galactosidase (Picard and Yamamoto, 1987).

The aequorin–GR chimeric cDNA was subcloned in the expression vector pEMSVscribe (Davis *et al.*, 1987) and transfected into HeLa cells together with the selectable plasmid pSV2neo (Southern and Berg, 1982). After G418 selection, 30 resistant clones were obtained and screened by

Northern analysis of aequorin mRNA expression (not shown). Clone #8 (N8) produced the highest amount of recombinant mRNA and was utilized in all the following experiments. The total amount of expressed protein (~ 0.2 ng/mg protein) was sufficient for *in situ* measurement of $[\text{Ca}^{2+}]_n$, though the signal to noise ratio was low, particularly under resting conditions. In order to enhance aequorin production, N8 cells were cultured for 24 h in the presence of 2 mM sodium butyrate, a compound known to activate recombinant gene expression in a number of model systems (Klehr *et al.*, 1992). This treatment dramatically increased the expression of recombinant aequorin: a Northern analysis of butyrate-treated and control N8 cells, demonstrates the marked enhancement of nuAEQ mRNA production (Figure 2). Accordingly, the total amount of aequorin, as measured after reconstitution *in vitro*, increased from 0.2 to 10 ng/mg protein, i.e. ~ 50 -fold. All the following experiments were thus performed with N8 cells pretreated for 24 h with butyrate; it should be, however, stressed that in all cases qualitatively similar results were obtained also with untreated cells.

Subcellular localization of recombinant aequorin

Attempts to determine the subcellular localization of the recombinant protein by immunofluorescence were unsuccessful, in as much as no specific signal was observed either in the nucleus or in the cytosol. Probably the relatively low amount of aequorin expressed and the poor immunogenicity of the protein both contributed to this unsuccessful result. Subcellular fractionation, according to

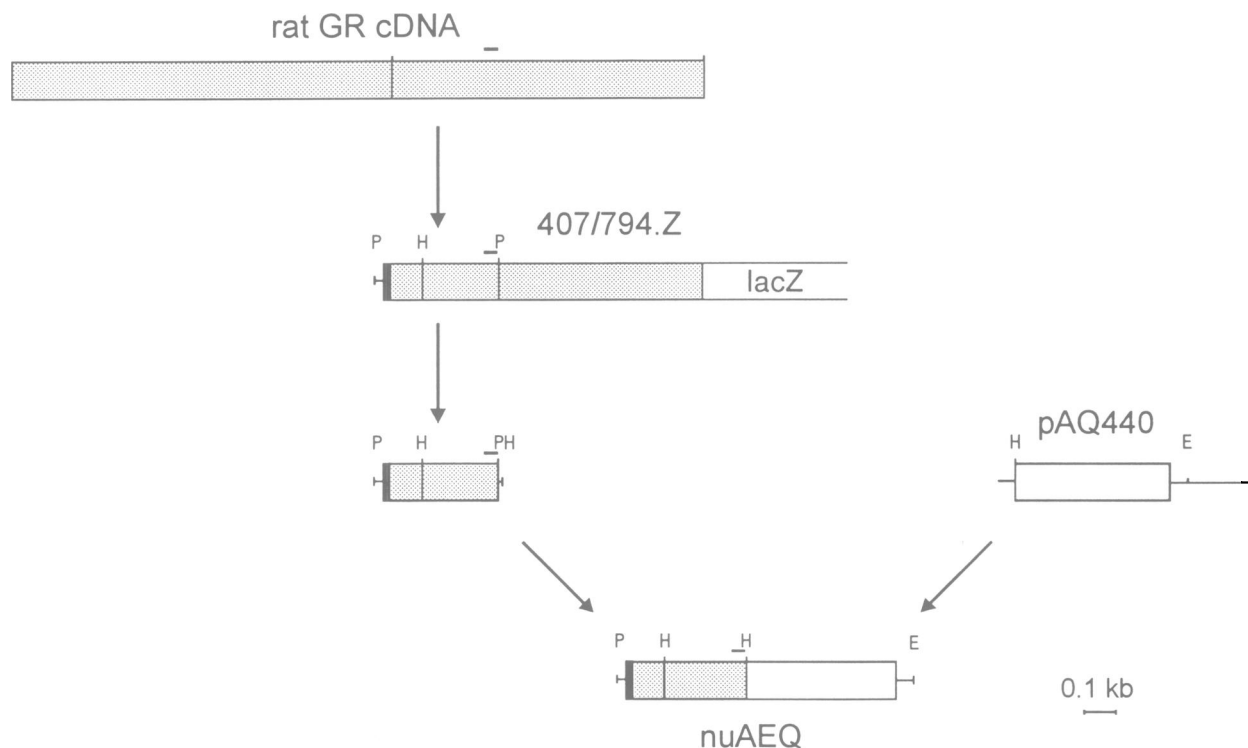


Fig. 1. Construction strategy of the chimeric aequorin–GR cDNA. pAQ440 (Inouye *et al.*, 1987) is the wild-type aequorin cDNA, including the whole coding region. A *PstI* fragment was excised from 407–794.Z (Picard and Yamamoto, 1987) and subcloned in PEX2 (this step allows the addition of a *HindIII* site in-frame with that of pAQ440 downstream of the GR cDNA). The two contiguous *PstI*–*HindIII* and *HindIII* fragments were ligated to the *HindIII*–*EcoRI* fragment of pAQ440, thereby generating the chimeric aequorin–GR cDNA denominated nuAEQ. Closed box, TK leader and AUG; shaded box, GR sequence (DNA binding domain + NL1), open box, aequorin cDNA. The restriction sites relevant to the construction are indicated (E, *EcoRI*; H, *HindIII*; P, *PstI*). The position of the nuclear localization signal NL1 is marked as a thick bar over the cDNA.

standard procedures, was excluded since NLSs are known to cause nuclear localization not because they bind firmly to nuclear structures, but because they mediate the transport of proteins across the nuclear pores (Garcia-Bustos *et al.*, 1991; Stochaj and Silver, 1992). During subfractionation the protein can be expected to leak out into the soluble supernatant. A different approach was thus used. Cells from clone N8 were treated with digitonin, a detergent preferentially affecting cholesterol-containing membranes, and the release in the supernatant of aequorin was compared with that of lactic dehydrogenase, LDH (a cytosolic marker). As shown in Figure 3A, 5 s after the application of digitonin, <2% of total aequorin, with respect to ~20% of LDH, was released in the supernatant. With time, however, also aequorin leaked out, as expected, and at the end of the experiment only ~50% was retained in the pellet. In order to rule out the possibility that spurious effects, such as the binding of aequorin to membranes or cytosolic structures, accounted for this difference, we have also analysed the release of the two proteins in a different HeLa clone (C4), which stably expresses unmodified (i.e. cytosolic) recombinant aequorin (M.Brini, unpublished). The data are presented in Figure 3B. The time course of digitonin permeabilization in the two clones was different; however, it is apparent that in clone C4 the release of aequorin closely paralleled that of the cytosolic marker. The direct comparison of the behaviour of the two aequorins is presented in Figure 3C, in which the ratio between released LDH and aequorin is plotted as a function of time. For cytosolic aequorin (cytAEQ), the ratio was < 1 at the first data points and then levelled at ~1. In contrast, in the case of nuclear-targeted aequorin (nuAEQ) the ratio was ~10 shortly after digitonin addition, decreasing with time and reaching ~1.7 after 2 min, as expected if aequorin is sequestered in a slowly equilibrating compartment. In particular, the values obtained

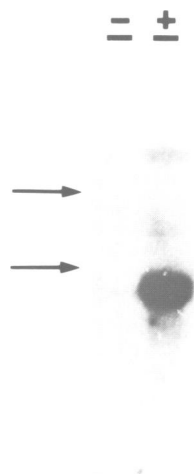


Fig. 2. Northern analysis of cells from clone N8, in the presence or absence of sodium butyrate. Total RNA was extracted from cells of clone N8, i.e. the highest producer among the HeLa clones isolated from the stable transfection with nuAEQ/pEMSVscribe and pSV2neo (see text). The RNA was electrophoresed, blotted and hybridized as described in Materials and methods. In the lanes marked +, the cells were incubated for 24 h with 2 mM sodium butyrate prior to RNA extraction; in the lanes marked -, sodium butyrate was omitted. Arrows indicate the position of ribosomal RNAs. The size of the hybridizing band (~900 nt) closely matches the prediction based on the dimensions of the chimeric cDNA.

at the earliest time after digitonin are likely to reflect more closely the situation of intact cells, suggesting that *in situ* recombinant aequorin is at least 10 times more concentrated in the nucleus than in the cytosol.

Admittedly, these results do not provide direct proof of the nuclear localization of chimeric aequorin, but the circumstantial evidence is very strong: (i) the recombinant protein is clearly located in a cellular compartment distinct from, but in passive equilibrium with, the cytosol; no organelle, but the nucleus, is known to possess such characteristics; (ii) the targeting sequence here employed has been previously shown to cause the selective, constitutive accumulation of a reporter protein in the nucleus (Picard and

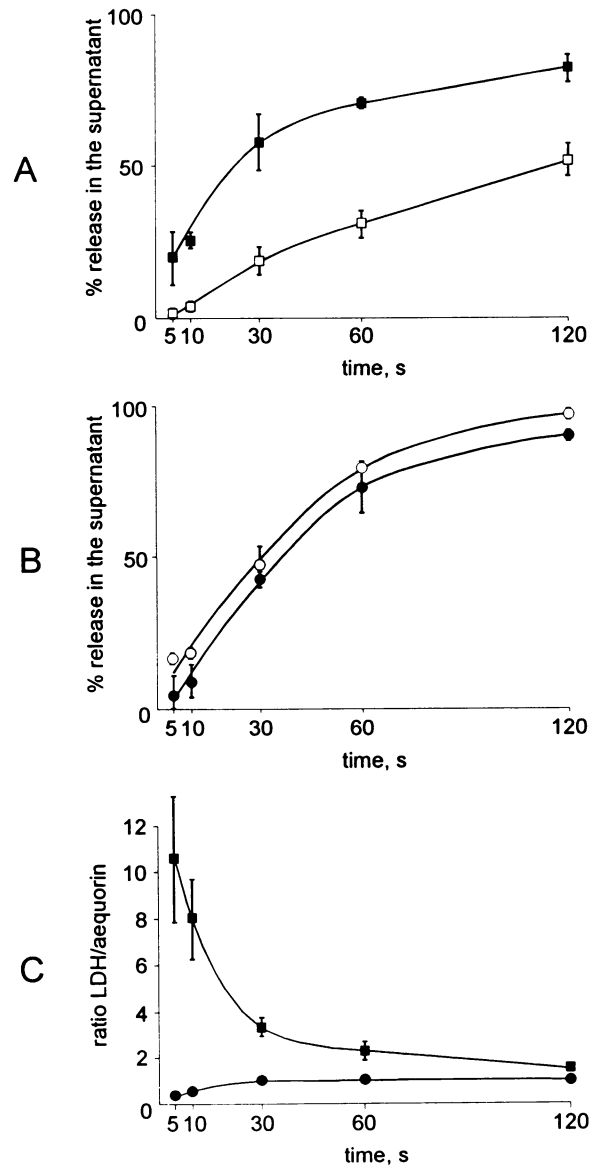


Fig. 3. Time course of aequorin and lactic dehydrogenase release following permeabilization of the plasma membrane with digitonin. Digitonin permeabilization, aequorin reconstitution and measurement and LDH enzymatic assay were as described in Materials and methods. Panels (A) and (B) show the absolute values (expressed as percent release) of clones N8 (nuclear-targeted aequorin, nuAEQ) and C4 (cytosolic aequorin, cytAEQ), respectively (open symbols, aequorin; closed symbols, LDH); panel (C) shows the ratio of LDH/aequorin (% total content) release in the two clones (squares, N8; circles, C4, as above). The results are the mean of five independent trials; where significant, the standard deviation is shown.

Yamamoto, 1987); and (iii) the $[Ca^{2+}]_n$ changes reported by the chimeric aequorin show significant differences from those measured with a cytosolic indicator (see below).

Measurements of $[Ca^{2+}]_n$ in intact cells

Figure 4 shows the measurements of aequorin luminescence in living cells, after *in situ* reconstitution of the active photoprotein with coelenterazine (Rizzuto *et al.*, 1992). Luminescence under resting conditions was hardly distinguishable from background level (Figure 4A); following the addition of histamine, an extracellular agonist coupled to the generation of inositol-1,4,5-trisphosphate (InsP3), light emission rapidly increased, reached the peak in ~ 8 s and then decreased to a slowly declining plateau level. Figure 4B presents the same data recalculated in terms of $[Ca^{2+}]_n$, assuming a nucleoplasmic ionic composition similar to that of the cytosol, i.e. pH 7.0 and 1 mM Mg^{2+} (Rink *et al.*, 1982). The resting $[Ca^{2+}]_n$ appears close to 100–200 nM; a large noise is, however, observed, as expected from the dose response curve of aequorin luminescence as a function of $[Ca^{2+}]$ (Blinks *et al.*, 1978; Thomas, 1982). Aequorin is, in fact, well suited for $[Ca^{2+}]$ measurements in the low micromolar range, but its sensitivity and accuracy sharply decrease when $[Ca^{2+}]$ is < 200 –300 nM. The rise in aequorin light emission caused by histamine corresponds to a mean $[Ca^{2+}]_n$ increase of $\sim 1.7 \mu M$ and $0.5 \mu M$, at the peak and during the plateau, respectively. Figure 4C shows the kinetics of $[Ca^{2+}]_i$, measured in parallel in a batch of the same cells loaded with fura-2. The kinetics of the $[Ca^{2+}]_i$ increase caused by histamine were very similar to those revealed by nuclear aequorin, though the peak and plateau were higher in the case of $[Ca^{2+}]_n$. Similar results were obtained with other InsP3-generating agonists, such as carbachol or ATP, though the amplitudes of $[Ca^{2+}]_i$ and $[Ca^{2+}]_n$ changes were smaller with these agonists than with histamine. The same results were also obtained with different clones or when a population of HeLa cells was transiently transfected and analysed (not shown), indicating that these observations are not specific to the tested clone N8.

The question then arises as to whether $[Ca^{2+}]_n$ is always in rapid equilibrium with $[Ca^{2+}]_i$ or whether conditions can be found in which $[Ca^{2+}]_n$ differs substantially from $[Ca^{2+}]_i$. In particular it can be hypothesized that if the origin of $[Ca^{2+}]_i$ increase is close to the nucleus, a transient higher increase in $[Ca^{2+}]_n$ could be generated. To test this possibility we took advantage of the fact that agonists, such as histamine, are coupled both to Ca^{2+} mobilization from intracellular stores (via InsP3 formation) and to Ca^{2+} influx, through activation of plasma membrane channels (Berridge, 1993). Cells were first incubated in Ca^{2+} -free medium supplemented with EGTA, to avoid any influx of Ca^{2+} from the medium, and then stimulated with histamine. Under this condition histamine caused a rapid increase both of aequorin (Figure 5A) and fura-2 (Figure 5C) signals. Addition of Ca^{2+} to the medium, in the continuous presence of the agonist, caused a second increase with both indicators. In the case of fura-2, the maximal $[Ca^{2+}]_i$ increases caused by intracellular release and influx were virtually identical, while in the case of aequorin, the difference in light output under the two conditions was dramatic, being > 5 -fold higher in the case of Ca^{2+} mobilization with respect to influx. Due to the square

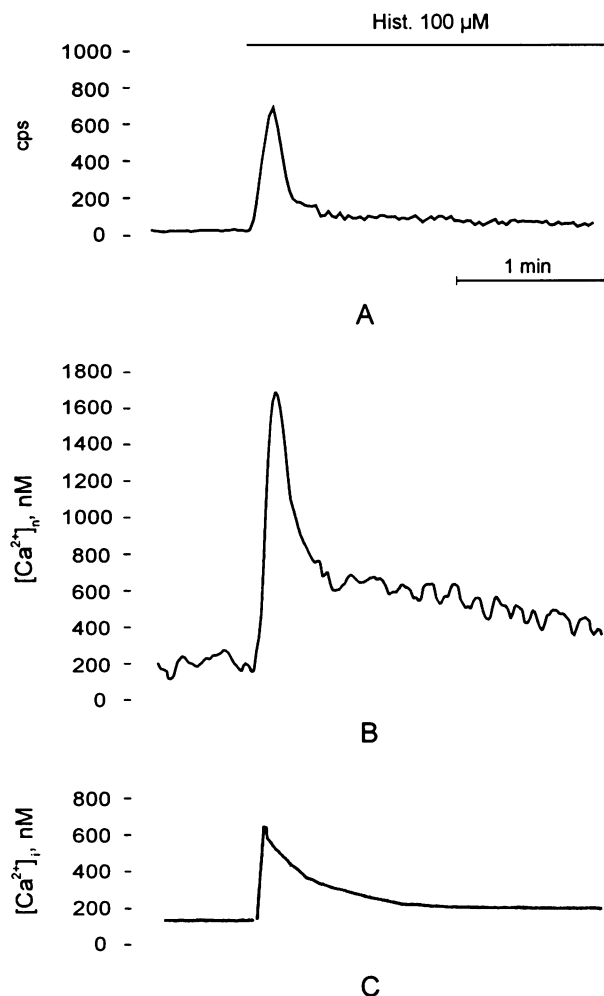


Fig. 4. $[Ca^{2+}]_i$ and $[Ca^{2+}]_n$ variations in clone N8 following stimulation with histamine. The cells were trypsinized, plated on glass coverslips and left in culture for 2 days. Loading with fura-2 and reconstitution with coelenterazine, as well as the calibration of the fluorescence and luminescence signals, were carried out as described in Materials and methods. Medium (modified Krebs–Ringer, KRB), in mM: 125 NaCl, 5 KCl, 1 Na_3PO_4 , 1 $MgSO_4$, 1 $CaCl_2$, 5.5 glucose and 20 HEPES (pH 7.4 at 37°C). Where indicated, 100 μM histamine was added. In aequorin measurements, cell lysis was obtained by exposing the cells to a hyposmotic, Ca^{2+} -rich solution. All reported experiments are representative of at least three different trials. (A) Aequorin luminescence in a monolayer of cells, in c.p.s. (B) $[Ca^{2+}]_n$ measurement, as derived from the luminescence data of panel A. (C) $[Ca^{2+}]_i$ measurement with fura-2 in a monolayer of cells.

relationship between aequorin luminescence and $[Ca^{2+}]$ (Blinks *et al.*, 1978), the difference in $[Ca^{2+}]_n$ rise in the two conditions was smaller than apparent from the crude luminescence data, but still quite evident (Figure 5B). A possible explanation of these results is that because of the characteristic response of aequorin to Ca^{2+} , the overall aequorin signal is dominated by the most responsive cells (Thomas, 1982). For example, if during Ca^{2+} redistribution from internal stores, 10% of the cells responded with a $[Ca^{2+}]_i$ increase 10-fold higher than the rest of the population, the mean aequorin signal would mainly reflect the $[Ca^{2+}]_n$ of this subpopulation. $[Ca^{2+}]_i$ was thus studied at the single cell level. Figure 5D shows the results of three typical cells stimulated with histamine. Despite the significant difference in the absolute $[Ca^{2+}]_i$ rises caused by the agonist in the three cells, within the same cell the amplitude

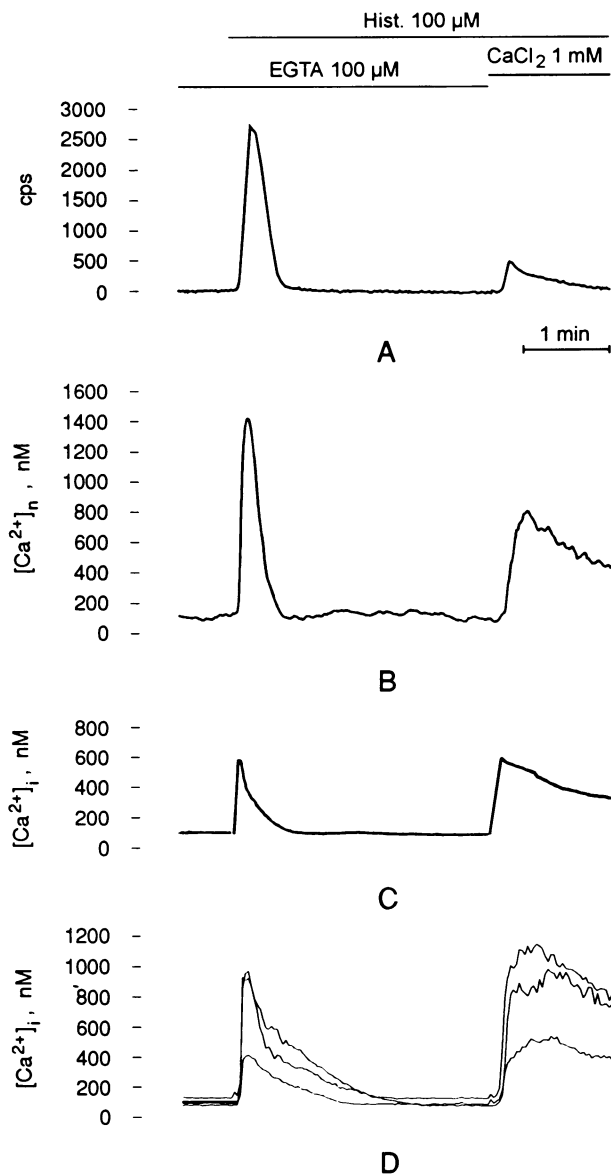


Fig. 5. Effect of histamine-induced Ca^{2+} mobilization and influx on $[Ca^{2+}]_i$ and $[Ca^{2+}]_n$. Conditions as in Figure 4, except that the initial medium did not contain $CaCl_2$. Where indicated, the medium was supplemented with $100 \mu M$ EGTA, $100 \mu M$ histamine and $1 mM$ $CaCl_2$. The first and the second peak reflect the contribution of InsP3-induced Ca^{2+} mobilization and Ca^{2+} influx from the external medium, respectively. (A) Aequorin luminescence in a monolayer of cells, in c.p.s. (B) $[Ca^{2+}]_n$ measurement, as derived from the luminescence data of panel A. (C) $[Ca^{2+}]_i$ measurement with fura-2 in a monolayer of cells. (D) $[Ca^{2+}]_i$ measurement with fura-2 in three representative cells. 100 individual cells were analysed in three separate experiments.

of the increases caused by Ca^{2+} mobilization and influx was very similar. Indeed, the $[Ca^{2+}]_i$ increase due to Ca^{2+} influx was identical or higher than that due to intracellular Ca^{2+} mobilization in 90 out of 100 single cells analysed. In the remaining 10 cells, although Ca^{2+} influx caused a $[Ca^{2+}]_i$ rise smaller than Ca^{2+} mobilization, this latter was within the range observed in the other cells. Taken together, the above described data demonstrate that the much larger nuclear signal evoked by Ca^{2+} mobilization compared with that evoked by Ca^{2+} influx cannot be attributed to a small proportion of highly responding cells, but rather to the fact that nuclear aequorin is exposed for a short period of time

to a $[Ca^{2+}]$ higher than that occurring in the bulk of the cytosol.

Discussion

Due to the role of Ca^{2+} in modulating key nuclear functions, the existence of nucleus/cytosol Ca^{2+} gradients at rest and upon stimulation has been the object of intense investigation. Using digital image analysis, several groups have reported differences between $[Ca^{2+}]_i$ and $[Ca^{2+}]_n$ both at rest and upon stimulation, suggesting that specific gating mechanisms or the activity of selective channels (see Mazzanti *et al.*, 1990) may allow a regulation of $[Ca^{2+}]_n$ at least in part independent from $[Ca^{2+}]_i$ (Williams *et al.*, 1985; Waybill *et al.*, 1991). Based on work on isolated nuclei, it has also been proposed that a distinct, ATP- and calmodulin-dependent Ca^{2+} uptake system causes a selective accumulation of Ca^{2+} inside the nucleus (Nicotera *et al.*, 1989). The existence of Ca^{2+} gradients between the nucleus and the cytoplasm has recently been challenged by Connor (1993), who demonstrated that such gradients can be observed only when the ester form of the dye is used and not when the dye is microinjected; he therefore suggested that the apparent gradients may be an artifact of the loading procedure. Our results provide the first measure of $[Ca^{2+}]_n$ utilizing a specific probe. Nuclear localization of targeted aequorin, although not directly shown by immunostaining, is supported by biochemical and functional evidence. In particular, the rates of release of nuclear and cytosolic aequorin induced by digitonin are clearly distinct (see Figure 3). We show that upon stimulation with InsP3-generating agonists, the $[Ca^{2+}]_i$ in the nucleus closely follows kinetically the behaviour of $[Ca^{2+}]_i$, suggesting that the nuclear membrane does not represent a major barrier to the diffusion of Ca^{2+} ions and that $[Ca^{2+}]_n$ does not possess an independent mechanism of regulation. As far as the resting values of $[Ca^{2+}]_i$ and $[Ca^{2+}]_n$ are concerned, they appear very close. Nonetheless, our data cannot exclude the possibility that small differences may indeed exist, given that $[Ca^{2+}]_i$ and $[Ca^{2+}]_n$ were measured with two different probes, whose calibration requires different assumptions. However, transiently expressed cytosolic and nuclear-targeted aequorin gave virtually identical resting values (R. Rizzuto, unpublished), confirming that also when the same Ca^{2+} probe is used, no nucleus-cytosol Ca^{2+} gradients can be seen in resting cells. Conversely, upon cell stimulation $[Ca^{2+}]_n$ reaches higher values than $[Ca^{2+}]_i$ (Figure 4). This cannot be attributed to the use of different probes, but appears to reflect a real phenomenon. In fact, independently of the absolute values, when Ca^{2+} redistribution and influx were experimentally separated (Figure 5), fura-2 revealed $[Ca^{2+}]_i$ increases of equal amplitude, while nuclear aequorin clearly showed a difference: $[Ca^{2+}]_n$ rises were larger when Ca^{2+} was mobilized from internal stores than when it entered from the external medium, suggesting that in the former case nuclear Ca^{2+} reveals the occurrence of InsP3-generated cytosolic gradients. This effect may depend on the presence of InsP3 receptors in the nuclear envelope (Ross *et al.*, 1989; Satoh *et al.*, 1990) and thus on the release of stored Ca^{2+} in the perinuclear space. Alternatively, it could simply reflect the spatial organization of the cell and in particular the close proximity to the nucleus of the endoplasmic reticulum cisternae acting as intracellular Ca^{2+} stores.

The different effect on the nucleus of $[Ca^{2+}]_i$ increases of different origins may have a major physiological role, especially in cells with a complex structural architecture, such as neurons. In these cells the Ca^{2+} signal is mediated by a number of channels and receptors, differing in their subcellular distribution, modulation and intracellular effects, and it can be speculated that the discrete distribution (e.g. cell body versus dendrites) and the properties of the Ca^{2+} channels may differentially affect $[Ca^{2+}]_n$ and, in turn, nuclear events. It has recently been shown that the activation of NMDA and non-NMDA ionotropic glutamate receptors has a markedly different effect on gene activation (Lerea and McNamara, 1993). The complexity of the spatial distribution of the $[Ca^{2+}]_i$ rises in the two cases (Bading *et al.*, 1993) and the possible generation of different nuclear-cytoplasm $[Ca^{2+}]$ gradients may play a crucial role in the control of this phenomenon.

Finally, although our data indicate that cytosolic and nucleoplasmic $[Ca^{2+}]$ most often rapidly equilibrate, situations may be envisaged in which the two signals may dissociate (e.g. during fertilization, a large increase in $[Ca^{2+}]_n$ has been hypothesized to occur, see Stricker *et al.*, 1992). The possibility of selectively monitoring $[Ca^{2+}]_n$, in these and other models, will now allow the direct investigation of the mechanism through which the agonist-induced variations of $[Ca^{2+}]_i$ are transduced to the nucleus and modulate processes of large biological and medical relevance, such as gene expression, apoptosis and excitotoxicity.

Materials and methods

Construction of nuAEQ cDNA

The start point for the construction of the chimeric cDNA was the plasmid GR 407-794.Z (Picard and Yamamoto, 1987). In this plasmid, a TK leader is fused in-frame with a portion of the rat GR, encoding the final 388 amino acids (407-794). A *Pst*I fragment, encoding the TK leader and amino acids 407-524 of the GR was subcloned in the PEX2 vector (Clontech). A *Hind*III site, present in this vector immediately downstream of the *Pst*I site, allowed the in-frame joining of the aequorin cDNA. The GR cDNA sequence was fused, by sequentially adding the *Pst*I-HindIII and the *Hind*III fragments to the aequorin cDNA (*Hind*III-EcoRI fragment of pAQ440, Inouye *et al.*, 1985), subcloned in the pBSK⁺ cloning vector (Stratagene). The construction strategy is summarized in Figure 1. The chimeric cDNA (nuAEQ), encoding the TK leader, amino acids 407-524 of the GR and the whole photoprotein, except the first amino acid, Val, was excised as a single *Eco*RI fragment and subcloned in the expression vector pEMSVscribe (Davis *et al.*, 1987). The cDNA construct was controlled by DNA sequencing; the orientation in the expression plasmid was verified by restriction mapping.

Cell culture

HeLa cells were grown in DMEM medium, supplemented with 10% fetal calf serum. The cells were currently grown on 75 cm² Falcon flasks; before transfection, cells were seeded onto Falcon 10 cm diameter Petri dishes. HeLa clone N8 was grown under the same conditions, but for the addition of G418 to the medium (see below). For fura-2 and aequorin measurements, the cells were plated onto appropriately sized glass coverslips (see below) two days before the experiment and grown in the absence of G418.

Transfection and selection of stable clones

HeLa cells were transfected with the calcium phosphate procedure, as described elsewhere by Sambrook *et al.* (1989), with a 9:1 ratio of nuAEQ/pEMSVscribe (see above) and pSV2neo (Southern and Berg, 1982), utilizing 40 µg of DNA for each 90 mm Petri dish. Two days after transfection, selection was started with 0.8 mg/ml G418; clones were visible after ~10 days and were isolated by selective trypsinization inside plastic cylinders (secured to the culture plate with sterile silicon). The clones were expanded into 75 cm² flasks and analysed by Northern blotting. After isolation, the G418 concentration in the medium was lowered to 0.2 mg/ml.

Screening of clones for aequorin production

Total RNA was extracted from each clone, using RNazol B (Biotec Laboratories Inc., Houston, TX) according to the protocol of the producing company. Northern analysis was performed according to standard procedures (Lehrach *et al.*, 1977), using 30 µg of total RNA per lane and random-prime labelled (Feinberg and Vogelstein, 1983) pAQ440 cDNA as a probe. The nylon membrane was washed at high stringency (4 × 30 min washes in 1 × SSC, 5% SDS, 10 mM sodium phosphate buffer pH 7.2 and 3 × 15 min washes in 0.5 × SSC, 0.1% SDS, all washes at 65°C) and exposed overnight for autoradiography with intensifying screen. (1 × SSC = 150 mM NaCl, 15 mM sodium citrate pH 7.6.)

Digitonin release of aequorin and LDH

Cells of clone N8 and of clone C4, which stably expresses cytosolic aequorin (M.Brini, unpublished), were plated on a 24-well plate 2 days before the experiment; aequorin was reconstituted with coelenterazine as described below. The DMEM medium and the excess coelenterazine were eliminated by washing the cells twice with a buffer containing, in mM: 130 KCl, 10 NaCl, 4 EGTA, 0.5 potassium phosphate buffer, 1 MgSO₄, 5 succinate, 5.5 glucose and 20 HEPES pH 7.0 at 37°C. The cells were then permeabilized in the same buffer containing 200 µM digitonin (Arslan *et al.*, 1985). Seventy microlitres of the supernatant were removed 5, 10, 30 and 60 s after the addition of digitonin and the remaining 120 µl after 120 s. At the end, the cells were dissolved in the same buffer containing 0.1% Triton X-100. The supernatants were cleared of cell debris by centrifugation (14 000 r.p.m. in an Eppendorf microcentrifuge). Aequorin luminescence was measured in a Packard Picolite A6100 luminometer after addition of 10 mM CaCl₂. LDH activity was measured spectrophotometrically (Arslan *et al.*, 1985).

Aequorin measurements

Our detection system was derived from that described by Cobbold and Lee (1991). In brief, the light emitted by aequorin is collected by a low noise photomultiplier, cooled to 4°C and the output is captured by an EMI C600 photon counting board installed in a microcomputer; a 13 mm-round coverslip with the cells is placed in a perfusion chamber (located immediately in front of the photomultiplier), which is thermostatted at 37°C via a waterbath and perfused via a Gilson Minipuls3 peristaltic pump. In our experiments, the recombinant photoprotein was reconstituted *in situ* by incubating the cells for 6-8 h with 2.5 µM coelenterazine in complete medium at 37°C before the experiment (Rizzuto *et al.*, 1992). The excess coelenterazine was washed away by perfusing the cells 1-2 min prior to recording. In order to obtain a rapid equilibration in the chamber, during the changes of medium the flow rate was increased from 2.5 to 6 ml/min. Under those conditions, 12 ± 1 s were necessary for the new medium to reach the chamber and 50% equilibration was obtained in 2 s. The luminescence data were off-line converted into $[Ca^{2+}]$ values by a program kindly provided by Dr R.Cuthbertson (University of Liverpool, UK). This program converts the computed fractional rate of consumption, derived from the raw data, into Ca^{2+} values on the basis of the known response curve of aequorin to Ca^{2+} at physiological conditions (Cobbold and Rink, 1987). The program also minimizes the effect of the background noise on basal values, by raising the time constant of the plot from 1 to 10 s at resting signals (i.e. <10 c.p.s.). The same results were obtained when a different calibration program (Rutter *et al.*, 1993) was employed. In all cases, for the calibration of the aequorin signal it is necessary to know L_{max} , i.e. the total amount of light that can be emitted by the active photoprotein. For this purpose, at the end of the experiment unconsumed aequorin was discharged by exposing the cells to a hyposmotic medium, containing only 10 mM CaCl₂.

Fura-2 measurements

For these experiments, the cells were grown on two types of coverslip, i.e. one 20 mm long and 8 mm wide for population studies, the other, for the single cell analysis, was round and 24 mm in diameter. Fura-2 loading was carried out as previously described by Malgaroli *et al.* (1987). In the population data, the coverslip was held in place of a multiwavelength fluorimeter, thermostatted at 37°C, which allows the analysis of a few thousand cells at a time, i.e. those illuminated by the incident beam. The excitation light passed through three filters (350, 360 and 380 nm) mounted in a computer-controlled rotating wheel. Emitted light was filtered through an interference filter centred at 500 nm. At the end of the experiment, 2 µM ionomycin and 1 mM Mn²⁺ were added to obtain the background signal. Calibration of the signal in terms of $[Ca^{2+}]_i$ was performed as described previously by Malgaroli *et al.* (1987). In the single cell experiments, the coverslip was placed in a thermostatted (37°C) chamber on the stage of an inverted fluorescence microscope (Zeiss Axiovert 100TV) connected to an imaging apparatus (Analytical Imaging Concepts, Atlanta,

USA). The sample was illuminated with a monochromatic beam (alternatively 340/380 nm) and the emitted light (filtered with an interference filter centred at 510 nm) collected by an intensified CCD camera (MTI). The output signal was processed by an imaging board and stored onto a Panasonic Videorecorder. The ratio images (1 ratio image/s) were calculated off-line, after background subtraction from each single image. The calculation of the background signal and the calibration were carried out as described above for the population. R_{\min} , R_{\max} and β were calculated *in situ* as described by Malgaroli *et al.* (1987).

Acknowledgements

We thank C. Bastianutto for help with some of the experiments and data analysis, G. Ronconi and M. Santato for technical assistance, Y. Kishi for the gift of coelenterazine, Y. Sakaki for the aequorin cDNA, P. Cobbold and R. Cuthbertson for the data analysis software and for advice in the construction of the aequorin detection system, G. Carmignoto, C. Montecucco, G. Schiavo and P. Volpe for critically reading the manuscript and G. F. Azzone for encouragement and support. This work was supported by grants from the Italian Research Council (CNR) 'Biotechnology' and 'Oncology', from 'Telethon', from the Italian Association for Cancer Research (AIRC) and from the 'AIDS project' of the Italian Health Ministry to T.P.

References

- Arslan, P., Di Virgilio, F., Beltrame, M., Tsien, R. Y. and Pozzan, T. (1985) *J. Biol. Chem.*, **260**, 2719–2727.
- Bading, H., Ginty, D. D. and Greenberg, M. E. (1993) *Science*, **260**, 181–186.
- Berridge, M. J. (1993) *Nature*, **361**, 315–324.
- Berridge, M. J. and Irvine, R. F. (1989) *Nature*, **341**, 197–205.
- Birch, B. D., Eng, D. L. and Kocsis, J. D. (1992) *Proc. Natl Acad. Sci. USA*, **89**, 7978–7982.
- Blinks, J. R., Mattingly, P. H., Jewell, B. R., van Leeuwen, M., Harrer, G. C. and Allen, D. G. (1978) *Methods Enzymol.*, **57**, 292–328.
- Cobbold, P. H. and Lee, J. A. C. (1991) In McCormack, J. G. and Cobbold, P. H. (eds), *Cellular Calcium, A Practical Approach*. IRL Press, Oxford, pp. 55–81.
- Cobbold, P. H. and Rink, T. J. (1987) *Biochem. J.*, **248**, 313–328.
- Collart, M. A., Tourkine, N., Belin, D., Vassalli, P., Jeanteur, P. and Blanchard, J.-M. (1991) *Mol. Cell. Biol.*, **11**, 2826–2831.
- Connor, J. A. (1993) *Cell Calcium*, **14**, 185–200.
- Davis, R. L., Weintraub, H. and Lassar, A. B. (1987) *Cell*, **51**, 987–1000.
- Feinberg, A. P. and Vogelstein, B. (1983) *Anal. Biochem.*, **132**, 6–13.
- Gaido, M. L. and Cidlowski, J. A. (1991) *J. Biol. Chem.*, **266**, 18580–18585.
- Garcia-Bustos, J., Heitman, J. and Hall, M. N. (1991) *Biochim. Biophys. Acta*, **1071**, 83–101.
- Grynkiewicz, G., Poenie, M. and Tsien, R. Y. (1985) *J. Biol. Chem.*, **260**, 3440–3450.
- Himpens, B., De Smedt, H., Droogmans, G. and Casteels, R. (1992) *Am. J. Physiol.*, **263**, C95–105.
- Inouye, S., Noguchi, M., Sakaki, Y., Takagi, Y., Miyata, T., Iwanaga, S., Miyata, T. and Tsuji, F. (1985) *Proc. Natl Acad. Sci. USA*, **82**, 3154–3158.
- Klehr, D., Schlake, T., Maass, K. and Bode, J. (1992) *Biochemistry*, **31**, 3222–3229.
- Lange, I., Scholz, M. and Peters, R. (1986) *J. Cell Biol.*, **102**, 1183–1190.
- Lehrach, H., Diamond, D., Wozney, J. M. and Boedtker, H. (1977) *Biochemistry*, **16**, 4743–4751.
- Lerea, L. S. and McNamara, J. O. (1993) *Neuron*, **10**, 31–41.
- Malgaroli, A., Milani, D., Meldolesi, J. and Pozzan, T. (1987) *J. Cell Biol.*, **105**, 2145–2155.
- Mazzanti, M., DeFelice, L. J., Cohen, J. and Malter, H. (1990) *Nature*, **343**, 764–767.
- Meldolesi, J., Madeddu, L. and Pozzan, T. (1990) *Biochim. Biophys. Acta*, **1055**, 130–140.
- Nicotera, P., McConkey, D. J., Jones, D. P. and Orrenius, S. (1989) *Proc. Natl Acad. Sci. USA*, **86**, 453–457.
- Nomura, M., Inouye, S., Ohmya, Y. and Tsuji, F. I. (1991) *FEBS Lett.*, **295**, 63–66.
- Picard, D. and Yamamoto, K. R. (1987) *EMBO J.*, **6**, 3333–3340.
- Rink, T. J., Tsien, R. Y. and Pozzan, T. (1982) *J. Cell Biol.*, **95**, 189–196.
- Rizzuto, R., Simpson, A. W., Brini, M. and Pozzan, T. (1992) *Nature*, **358**, 325–327.
- Ross, C. A., Meldolesi, J., Milner, T. A., Satoh, T., Supattapone, S. and Snyder, S. H. (1989) *Nature*, **339**, 468–470.
- Rutter, G. A., Theler, J.-M., Murgia, M., Wollheim, C. B., Pozzan, T. and Rizzuto, R. (1993) *J. Biol. Chem.*, in press.
- Sambrook, J., Fritsch, E. F. and Maniatis, T. (1989) *Molecular Cloning, A Laboratory Manual*. Second Edition. Cold Spring Harbor Laboratory Press, Cold Spring Harbor, NY.
- Satoh, T., Ross, C. A., Villa, A., Supattapone, S., Pozzan, T., Snyder, S. H. and Meldolesi, J. (1990) *J. Cell Biol.*, **111**, 615–624.
- Southern, P. J. and Berg, P. (1982) *J. Mol. Appl. Genet.*, **1**, 327–341.
- Stochaj, U. and Silver, P. (1992) *J. Cell Biol.*, **117**, 473–482.
- Stricker, S. A., Centonze, V. E., Paddock, S. W. and Schatten, G. (1992) *Dev. Biol.*, **149**, 370–380.
- Thomas, M. V. (1982) *Techniques in Calcium Research*. Academic Press, London.
- Tombes, R. M., Simerly, C., Borisy, G. G. and Schatten, G. (1992) *J. Cell Biol.*, **117**, 799–811.
- Tsien, R. Y. (1989) *Annu. Rev. Neurosci.*, **12**, 227–253.
- Tsien, R. Y., Pozzan, T. and Rink, T. J. (1982) *J. Cell Biol.*, **94**, 325–334.
- Waybill, M. M. *et al.* (1991) *Am. J. Physiol.*, **261**, E49–E57.
- Williams, D. A., Fogarty, K. E., Tsien, R. Y. and Fay, F. S. (1985) *Nature*, **318**, 558–561.

Received on June 15, 1993; revised on August 5, 1993